ISSN 0915-633X

NATIONAL INSTITUTE FOR FUSION SCIENCE

Multi-Scale Semi-Ideal Magnetohydrodynamics of a Tokamak Plasma

S. Bazdenkov, T. Sato, K. Watanabe and
The Complexity Simulation Group

(Received - Sep. 6, 1995)

NIFS-376 Sep. 1995

RESEARCH REPORT
NIFS Series

NAGOYA, JAPAN

MULTI-SCALE SEMI-IDEAL MAGNETOHYDRODYNAMICS OF A TOKAMAK PLASMA

Sergey Bazdenkov, Tetsuya Sato, Kunihiko Watanabe

and The Complexity Simulation Group[1]

Theory and Computer Simulation Center

National Institute for Fusion Science, Nagoya 464-01, Japan

Abstract

An analytical model of fast spatial flattening of the toroidal current density and q-profile at the nonlinear stage of $(m = 1/n = 1)$ kink instability of a tokamak plasma is presented. The flattening is shown to be an essentially multi-scale phenomenon which is characterized by, at least, two magnetic Reynolds numbers. The ordinary one, R_m, is related with a characteristic radial scale-length , while the other, R_m^*, corresponds to a characteristic scale-length of plasma inhomogenety along the magnetic field line. In a highly conducting plasma inside the $q = 1$ magnetic surface, where q value does not much differ from unity, plasma evolution is governed by a multi-scale non-ideal dynamics characterized by two well-separated magnetic Reynolds numbers, R_m and $R_m^* \equiv (1 - q)\ R_m$, where $R_m^* \sim O(1)$ and $R_m \gg 1$. This dynamics consistently explains two seemingly contradictory features recently observed in a numerical simulation [Watanabe et al., 1995]: i) the current profile (q-profile) is flattened in the magnetohydrodynamic time scale within the $q = 1$ rational surface; ii) the magnetic surface keeps its initial circular shape during this evolution.

Keywords: tokamak, fast current profile flattening, multi-scale semi-ideal MHD.

---

[1]R.Horiuchi, T.Hayashi, Y.Todo, A.Kageyama, T.H.Watanabe and H.Takamaru

I. INTRODUCTION

Recent numerical simulation by Watanabe et al.[1] has revealed an interesting but puzzling phenomenon associated with nonlinear evolution of a resistive kink mode ($m = 1/n = 1$) instability. While the magnetic surface keeps its almost initial circular structure, the toroidal current density profile, hence, the q-profile, is flattened within the $q = 1$ surface in the magnetohydrodynamic (MHD) time scale (Fig.1, or see Fig.2 of [1]). It is also found that while the magnetic surface obtained by mapping a successive intersection point of a magnetic field line on a poloidal plane keeps its initial circular structure (Fig.2a), the toroidal current suffers an appreciable $m = 1/n = 1$ helical kink deformation (Fig.2b) due to a strongly excited $m = 1/n = 1$ kink flow (Fig.2c). These seemingly intriguing and contradictory observations in the numerical simulation invoke us to search for a fast diffusion time scale other than the simple classical resistive time scale.

As the length scale that governs the non-ideality of an MHD plasma, we can conceive two scales, one being the perpendicular (radial in the present case) scale of the plasma inhomogeneity, r_s, which is, e.g. the radius of $q = 1$ surface, and the other the parallel inhomogeneity length, $l_{\|} = \dfrac{|\mathbf{B}|}{|\mathbf{B}\cdot\nabla|}$. The perpendicular length r_s is conventionally used for defining the resistive time scale and the MHD (Alfven) time scale, thus, the magnetic Reynolds number R_m.

In an ideal case, a magnetic field line is always on the same "ideal", i.e., frozen into a plasma flow, magnetic surface $\psi_m = const$, so that $(\mathbf{B}\cdot\nabla)\psi_m = 0$. In the presence of resistivity η, however, $(\mathbf{B}\cdot\nabla)\psi_m \sim O(\eta)$, and the parallel scale length $l_{\|}$ will be finite, not infinite as is so for an ideal plasma. In a helically ($m = 1/n = 1$) disturbed resistive plasma, no matter how small the resistivity may be, the effective parallel scale length will be increased by a factor $(1-q)^{-1}$. As the change of ψ_m along $\mathbf{B}$ is proportional to $l_{\|}$ and corresponds to a magnetic field line transition from one $\psi_m = const$ surface to another, the effective magnetic Reynolds number near the $q = 1$ surface, R_m^*, will be modified to

$R_m^* \approx (1-q)R_m$. Therefore, the R_m^* will be drastically reduced near the $q = 1$ surface. This reduction may probably explain an experimentally observed change of q-profile on a time scale much shorter than the ordinary magnetic diffusion time [2-4]. However, the physics of the sawtooth crash in a tokamak plasma (there exists considerable literature on this subject, see e.g. the review [5] and references therein) is not considered in the present paper. We are rather aimed to explain the numerically revealed phenomenon [1] whose nature, probably, is closely related with the sawtooth crash.

In this paper we give a physical background of a multi-scale semi-ideal MHD phenomenon. The zero-beta limit and cylindrical geometry are considered. However, the results are qualitatively applicable to the more general case of the finite pressure and non-cylindrical geometry. The paper is organized in the following way. In Section 2 a multi-scale semi-ideal MHD approach is developed. First of all, in Subsection 2.1 the problem of how a magnetic field line slips from a low-resistive plasma flow is considered. The slipping is shown to be controlled by two important factors: i) an "effective" length of the field line, $l_{\|} \sim r_s \mid \frac{B_\vartheta}{B} \mid (1-q)^{-1}$, instead of a characteristic radial scale length r_s, and ii) dissipative coupling of the radial and poloidal components of the magnetic field (this geometric effect is underestimated in most previous considerations). The $(1-q)$ - factor reduces a flow-induced radial shift of the magnetic field line, while the geometric coupling effect enhances a resistive perturbation of radial magnetic field. As a result, the slipping is shown to be controlled by the modified magnetic Reynolds number $R_m^* = (1-q)\ R_m$ which can become much smaller than R_m . We regard such a situation that $R_m^* \ll R_m$ as the semi-ideal magnetohydrodynamics. There are many different kinds of magnetic configuration and plasma flow governed by this semi-ideal MHD. But we are here interested in a particular nonlinear evolution with undisturbed magnetic surfaces, i.e., with $B_r \approx 0$, like in [1]. Conditions under which the assumption $B_r = 0$ is consistent with the nonlinear MHD equations are analyzed in Subsection 2.2. The corresponding semi-ideal MHD ordering is discussed. Then, in Section 3, the multi-scale semi-ideal MHD equations are derived which describe the fast q - profile deformation at the nonlinear stage of kink instability. The problem is reduced to coupling of the toroidally averaged poloidal component of magnetic field with the radial distribution of the R_m^* value which is closely related with local $l_{||}$ value. Conclusions are summarized in Section 4.

2. SEMI-IDEAL MHD APPROACH

Let us consider the simple Ohm's law:

$$\mathbf{E} + [\mathbf{V} \times \mathbf{B}] = \eta \mathbf{j}, \tag{1}$$

where η is a resistivity. Faraday's law takes the form:

$$\frac{\partial \mathbf{B}}{\partial t} = rot([\mathbf{V} \times \mathbf{B}] - \eta \mathbf{j}). \tag{2}$$

It is well known that in the presence of resistivity, magnetic field is not frozen into plasma flow and slips from it. The slipping is usually thought to be controlled by a simple perpendicular diffusion, $\dfrac{\partial B}{\partial t} = \dfrac{\eta}{\mu_0}\Delta B \sim -(\dfrac{\eta}{\mu_0 r_s^2})B$. But actually the slipping is a complicated phenomenon that includes a non-trivial interaction between a driving force (plasma flow) and a dissipative effect in a plasma confined by closed magnetic surfaces.

2.1. Unfrozen magnetic field.

Multiplying Eq.(2) by a gradient of arbitrary scalar function $\nabla\psi$ and carrying out some mathematical manipulation one obtains:

$$\frac{\partial}{\partial t}(\mathbf{B} \cdot \nabla\psi) + div(\mathbf{V}(\mathbf{B} \cdot \nabla\psi)) - (\mathbf{B} \cdot \nabla)(\frac{\partial}{\partial t} + \mathbf{V} \cdot \nabla)\psi = -(\nabla\psi \cdot rot(\eta \mathbf{j})). \tag{3}$$

Let ψ be frozen into plasma flow,

$$(\frac{\partial}{\partial t} + \mathbf{V} \cdot \nabla)\psi = 0, \tag{4}$$

i.e., ψ is a function of the Lagrange coordinates. In this case, Eq.(3) can be written as

$$(\frac{\partial}{\partial t} + \mathbf{V} \cdot \nabla)\frac{(\mathbf{B} \cdot \nabla\psi)}{\rho} = -\frac{1}{\rho}\,(\nabla\psi \cdot rot(\eta\mathbf{j})). \tag{5}$$

Here ρ is the plasma density obeying the continuity equation

$$\frac{\partial\rho}{\partial t} + div(\rho\mathbf{V}) = 0. \tag{6}$$

In the case of ideal plasma with $\eta = 0$ Eq.(5) describes the freezing of $\frac{1}{\rho}(\mathbf{B} \cdot \nabla\psi)$ into the plasma flow. It means that if ψ is initially constant along a field line, i.e. $(\mathbf{B} \cdot \nabla\psi) = 0$ everywhere, then the line is lying on a $\psi = const$ surface, and this property remains at any time. As ψ is frozen into a flow (see Eq.(4)), a magnetic surface, i.e., a $\psi = const$ surface, is frozen into the ideal MHD plasma flow.

In the case of resistive medium, Eq.(5) contains a source term on its right-hand-side (r.h.s.) leading to a non-constancy of ψ along a magnetic field line. The change of ψ along $\mathbf{B}$ corresponds to a magnetic field line transition from one $\psi = const$ surface frozen into a plasma flow to another, $\psi + \delta\psi = const$ surface. Within a time scale of the order of τ_{MHD} this change is proportional to

$$\delta\psi \;\sim\; \tau_{MHD}\,(\mathbf{B} \cdot \nabla)^{-1}(\nabla\psi \cdot rot(\eta\mathbf{j})) \;\sim\; \frac{\eta l_{\|}\,\tau_{MHD}}{B}\,(\nabla\psi \cdot rot\mathbf{j}), \tag{7}$$

where $l_{\|}$ is a characteristic length of inhomogenety along the field lines and $\tau_{MHD} \equiv \frac{r_s}{V_{Ap}}$ is a characteristic time scale of magnetic structure deformation by plasma flow, V_{Ap} being the Alfven velocity defined by the poloidal magnetic field. Plasma density ρ and resistivity η are assumed to be constant. Non-constancy of η may lead to some interesting effects which, however, we do not consider in the present paper.

In Eq.(7), $\delta\psi$ represents a magnetic field line shift in the Lagrange frame. The corresponding shift in the Euler frame can be estimated as

$$\delta r \approx \frac{\delta\psi}{\mid \nabla\psi \mid} \;\sim \mid \frac{\eta l_{\|}\,\tau_{MHD}}{B}\,(rot\mathbf{j})_r \mid . \tag{8}$$

Here $\nabla\psi$ represents a generalized "radial" direction perpendicular to $\psi = const$ surface (we assume that the surface is topologically equivalent to a cylinder) and $(rot\mathbf{j})_r$ is the radial component of $rot\mathbf{j}$ perpendicular to the $\psi = const$ surface. Since we are interested in a resistive breakdown of the freezing of magnetic field into plasma flow, it is quite reasonable to assume that initial ψ corresponds to the initial distribution of magnetic flux. So, the $\psi = const$ surface is just the "ideal" magnetic surface deformed by plasma flow, while $\delta\psi$ or δr describes a magnetic field line slippage from this "ideal" surface in the presence of resistivity.

This slippage, in accordance with the expression (8), depends on $(rot\mathbf{j})_r$ which, at first glance, is scaled by $\frac{B_r}{r_s^2}$ (according to [1], nor inertial neither resistive singular layer [6] exists within $q = 1$ surface at the nonlinear stage of $m = 1, n = 1$ kink instability). The truth, however, is that $(rot\mathbf{j})_r$ is controlled by a geometrical effect (coupling of the poloidal and toroidal harmonics of the radial and poloidal magnetic fields) that would change drastically the physics of the slippage. Note that this important effect is underestimated in most previous considerations. Indeed, in a cylindrical geometry, which is quite natural in the case of tokamak plasma, the radial component of $rot\ \mathbf{j}$ is determined by both the radial and poloidal components of magnetic field, if the system is poloidally inhomogeneous. Namely, one has exactly:

$$(rot\mathbf{j})_r = \frac{1}{\mu_0}(rot\ rot\mathbf{B})_r = \frac{1}{\mu_0}\left[-\Delta B_r + \frac{1}{r^2}\left(B_r + 2\frac{\partial B_\vartheta}{\partial\vartheta}\right)\right], \qquad (9)$$

where $\Delta \equiv \frac{1}{r}\frac{\partial}{\partial r}(r\frac{\partial}{\partial r}) + \frac{1}{r^2}\frac{\partial^2}{\partial\vartheta^2} + \frac{\partial^2}{\partial z^2}$.

Eq.(9) indicates that the poloidal and toroidal (along the z-direction) harmonics of B_r and B_ϑ are coupled. So, during a purely dissipative evolution described by Eq.(2) with $\mathbf{V} \equiv 0$ the radial component of magnetic field can be generated, even though absent initially. Generally, dissipative perturbations of B_r can be significantly enhanced because of the geometrical effect described by the last term in Eq.(9), i.e., $(rot\mathbf{j})_r \approx \frac{2}{\mu_0 r^2}\frac{\partial B_\vartheta}{\partial\vartheta}$

(such an enhancement qualitatively differs from a primitive increase of the operator Δ in a singular layer). Substituting this expression into Eq.(8) one obtains:

$$\frac{\delta r}{r_s} \approx (\frac{\tau_{MHD}}{\tau_\eta})\,(\frac{2l_\parallel}{r_s})\,(\frac{r_s}{r})^2 \mid \frac{1}{B}\,\frac{\partial B_\vartheta}{\partial \vartheta} \mid, \qquad (10)$$

where $\tau_\eta = \frac{\mu_0 r_s^2}{\eta}$ is the ordinary resistive time scale. The quantity $\frac{l_\parallel}{r_s}$ in Eq.(10) can be estimated as $\frac{r_s}{l_\parallel} \approx r_s \mid \frac{(\mathbf{B}\cdot\nabla)}{B} \mid \approx \mid \frac{B_\vartheta}{B} \mid (\frac{\partial}{\partial\vartheta} + \frac{B_z}{B_\vartheta} r_s \frac{\partial}{\partial z}) \approx (1-q) \mid \frac{B_\vartheta}{B} \mid$ for $m = 1/n = 1$ mode (here $(1-q)$ just measures the angle between field line and symmetry direction of the mode). Then we obtain

$$\frac{\delta r}{r_s} \approx \frac{2\,(\frac{\tau_{MHD}}{\tau_\eta})\,(\frac{r_s}{r})^2}{\mid 1-q \mid} \approx \frac{2}{R_m \mid 1-q \mid}. \qquad (11)$$

In the region where $\mid 1-q \mid \sim O(1)$, this quantity reduses to $\frac{2}{R_m}$ which describes the ordinary diffusion. In the region of $q \approx 1$, however, the resistive slippage of a magnetic field line, δr, can be enormously enhanced. This indicates that the diffusion effect may become comparable to the MHD effect. Hence, the actual resistive diffusion should be characterized by a parameter R_m^* which is defined by $R_m \mid 1-q \mid$ instead of ordinary Reynolds number R_m. Even though the R_m value is large, the parameter R_m^* can become very small, say, of the order of unity, so a field line can be shifted from the "ideal" (i.e., frozen into the plasma flow) magnetic surface by a substantial distance. That the dissipative unfreezing of the magnetic field from plasma flow is controlled by the modified Reynolds number R_m^*, instead of the conventional one, is a general result, which plays a key role in the semi-ideal MHD.

Note, that in the present paper we consider namely the enhancement of reconnection (unfreesing) due to smallness of $1-q$. This should not be mixed with an other, quite different effect which is related with the smallness of $1-q$ as well (see the paper by Wesson [7]). Wesson [7] shows that in a system with small $1-q$ an ideal $m=1$ kink instability can produce rearrangement of $q-$ profile on an inertial, i.e., fast time scale.

But the reconnection does not occur during this rearrangement at all (this is especially emphasised in Wesson's paper). Hence, a plasma flow generated by the instability should strongly disturb a magnetic surface - exactly the opposite of what the numerical simulation by Watanabe et al [1] has revealed and what we are aimed to explain in the present paper.

2.2. Semi-ideal MHD ordering.

Since we are interested in such a particular flow that magnetic surfaces could maintain their circular shape, without being disturbed by plasma flow, even in the case of low-resistive plasma with $R_m \gg 1$, we wish to derive the conditions under which the assumption $B_r = 0$ is consistent with the governing MHD equations, namely, cancellation between the dissipative and flow-induced perturbations of radial magnetic field. So, we rather answer the question - When does the flow with (assumed) $B_r = 0$ exist? - instead of - Why $B_r = 0$? The condition $B_r = 0$ can not be derived from the general principles just because such a condition is not a general property of MHD flows at all. Vice versa, the flow with $B_r = 0$ is rather a conditional flow which can be realized only in a special case of semi-ideal MHD ordering considered below. Of course, a magnetic configuration does not always obey this ordering. But if it obeys then the flow with $B_r = 0$ can exist during a considerable period of time. Therefore, assuming $B_r = 0$, we just specify a particular solution of interest among an infinite set of other, quite different solutions of MHD equations. After that we find the conditions when such a solution is consistent with the governing equations and, hence, can be realized on a sufficiently long time scale.

In order to compare each term in Eq.(2) it is useful to introduce dimensionless variables:

$$x = \frac{r}{r_s}; \ \alpha = \frac{2\pi z}{z_0}; \ \tau = \frac{t}{\tau_{MHD}} = \frac{t\,V_{Ap}}{r_s}; \ \mathbf{u} = \frac{\mathbf{V}}{V_{Ap}}; \ \mathbf{b} = \frac{\mathbf{B}}{B_0}, \tag{12}$$

where B_0 is the unperturbed value of toroidal magnetic field; r_s is the radius of initial $q = 1$ surface; z_0 is the length of a periodical cylinder; the Alfven velocity V_{Ap} is defined by the initial poloidal magnetic field at $r = r_s$, i.e., $B_{\vartheta 0} = B_0 \frac{2\pi r_s}{z_0}$.

Corresponding dimensionless form of each component of Eq.(2) is given by

$$\frac{\partial b_r}{\partial \tau} + \nabla (b_r \, \mathbf{u}) = (\mathbf{b}\nabla) u_r + \frac{1}{R_m} \, [\, \Delta b_r \, - \, \frac{1}{x^2} \, (b_r + 2 \, \frac{\partial b_\vartheta}{\partial \vartheta})], \tag{13}$$

$$\frac{\partial}{\partial \tau} (\frac{b_\vartheta}{x}) + \nabla (\frac{b_\vartheta}{x} \, \mathbf{u}) = (\mathbf{b}\nabla) \frac{u_\vartheta}{x} + \frac{1}{R_m} \, \frac{1}{x} \, [\, \Delta b_\vartheta \, - \, \frac{1}{x^2} \, (b_\vartheta - 2 \, \frac{\partial b_r}{\partial \vartheta})], \tag{14}$$

$$\frac{\partial b_z}{\partial \tau} + \nabla (b_z \, \mathbf{u}) = (\mathbf{b}\nabla) u_z + \frac{1}{R_m} \, \Delta b_z, \tag{15}$$

where $\Delta \equiv \frac{1}{x}\frac{\partial}{\partial x}(x\frac{\partial}{\partial x}) + \frac{1}{x^2}\frac{\partial^2}{\partial \vartheta^2} + (\frac{B_{\vartheta 0}}{B_0})^2 \frac{\partial^2}{\partial \alpha^2}$, $\nabla \equiv (\frac{\partial}{\partial x}; \; \frac{1}{x}\frac{\partial}{\partial \vartheta}; \; \frac{B_{\vartheta 0}}{B_0}\frac{\partial}{\partial \alpha})$ and $R_m = \frac{\tau_\eta}{\tau_{MHD}}$. From Eq.(13) it follows that in the main order of power expansion of b_r (we assume $b_r \to 0$), dissipative, $\frac{2}{R_m \, x^2} \frac{\partial b_\vartheta}{\partial \vartheta}$, and flow-induced, $(\mathbf{b} \cdot \nabla) u_r \approx \mid b_\vartheta \mid \; (1-q) \, \frac{\partial u_r}{\partial \vartheta}$, perturbations of radial magnetic field should be balanced, i.e.,

$$\tilde{b_\vartheta} = \frac{x}{2} \, (1-q) \, R_m \, \tilde{u_r} \;\; < b_\vartheta >, \tag{16}$$

where $\tilde{b_\vartheta}$ and $\tilde{u_r}$ are poloidally varying parts of b_ϑ and u_r , while $< b_\vartheta >$ is the poloidally averaged one. In the nonlinear stage of kink instability, helical perturbations are large, i.e., $\mid \tilde{b_\vartheta} \mid \approx \mid < b_\vartheta > \mid$ and $\mid \tilde{u_r} \mid \approx 1$, so that Eq.(16) yields

$$(1-q) \; R_m \equiv R_m^* \sim O(1). \tag{17}$$

At the same time, the condition that the terms containing b_r in Eq.(13) be much less than the above two terms, dissipative and flow-induced ones, must be satisfied, namely,

$$\mid b_r \mid \ll (1-q) \;\; \mid b_\vartheta \mid . \tag{18}$$

Of course, the relationship (16) between $\tilde{b_\vartheta}$ and $< b_\vartheta >$ has to be consistent with the formal equation for $\tilde{b_\vartheta}$ (i.e. with the poloidally varying part of Eq.(14)) at the semi-ideal limit:

$$R_m \to \infty, \;\; (1-q) \to 0, \;\; R_m^* \sim O(1). \tag{19}$$

Substitution of Eq.(16) into Eq(14) yields that the terms $\frac{4\ \tilde{u}_r}{R_m^* \ < b_\vartheta >} \frac{\partial}{\partial x}(\frac{< b_\vartheta >}{x})$ and $\frac{\partial \tilde{u}_r}{\partial \tau}$ be balanced (here $\frac{\partial \tilde{u}_r}{\partial \tau}$ follows formally from the time-derivative of Eq.(16); the consistency of Eqs.(16) and (14) demands the term $\frac{\partial \tilde{u}_r}{\partial \tau}$ should not be arbitrary). On the other hand, the acceleration term $\frac{\partial \tilde{u}_r}{\partial \tau}$ is known to be related with the $[\ \mathbf{j} \times \mathbf{B}\ ]$ force in the radial component of momentum equation. In dimensionless variables this acceleration term can be written as $\mid \frac{\partial \tilde{u}_r}{\partial \tau} \mid \approx (\frac{B_0}{B_{\vartheta 0}})^2 \ R_m^* \ < b_\vartheta >^2 \mid \tilde{u}_r \mid$, where $\tilde{b_\vartheta}$ in Eq.(16) is substituted. Comparing these two $\mid \frac{\partial \tilde{u}_r}{\partial \tau} \mid$ terms, therefore, one finds that the relationship (16) is consistent with both the formal equation for $\tilde{b_\vartheta}$ (poloidally varying part of Eq.(14)) and the r-component of momentum equation within a small relative error of $R_m^* \ < b_\vartheta >$ of the order of $O((\frac{B_{\vartheta 0}}{B_0})^2)$, when

$$(\frac{B_{\vartheta 0}}{B_0})^2 = (\frac{2\pi r_s}{z_0})^2 \ll 1. \tag{20}$$

The consistency of Eqs.(16) and (14) can be explained as follows: during the evolution of a kink mode, $\mathbf{j}$ and $\mathbf{B}$ vectors are approximately parallel to each other, i.e. $\mid [\ \mathbf{j} \times \mathbf{B}\ ] \mid \ll \mid \mathbf{j} \mid \mid \mathbf{B} \mid$, hence, the error in the acceleration term can be compensated by a small change of the angle between the magnetic field and current density vectors.

Thus, one can conclude that the evolution of magnetic structure with practically undisturbed magnetic surfaces can be, without inconsistency, realized by the governing equation (2), if the semi-ideal orderings (18), (19) and (20) are satisfied.

3. MULTI-SCALE MODEL EQUATIONS

We shall now derive the governing equations that describe the process of fast q-profile deformation and magnetic configuration with circular magnetic surfaces in the nonlinear stage of kink instability in the semi-ideal limit.

For simplicity but without any loss of generality we consider a helically symmetric magnetic configuration described by two independent dimensionless (see Eq.(12)) variables, helical magnetic flux a_h and poloidal magnetic field b_ϑ. For the case where magnetic surfaces keep their initial circular shape, i.e., $b_r \equiv 0$, one can write:

$$b_r = -\frac{1}{x}\frac{\partial a_h}{\partial \xi} = 0, \tag{21}$$

$$b_\vartheta - \epsilon x b_z = \frac{\partial a_h}{\partial x}, \tag{22}$$

where $\epsilon = \dfrac{2\pi r_s}{z_0}$ is a "toroidicity", and the "helical" angle

$$\xi = \vartheta - \frac{2\pi}{z_0} z \tag{23}$$

corresponds to helical symmetry of the most unstable ($m = 1/n = 1$) mode, so that $\dfrac{\partial}{\partial\vartheta} \equiv \dfrac{\partial}{\partial\xi}$ and $\dfrac{\partial}{\partial z} \equiv -\dfrac{2\pi}{z_0}\dfrac{\partial}{\partial\xi}$. In the same notation, operator $(\mathbf{b}\cdot\nabla)$ has the form

$$(\mathbf{b}\cdot\nabla) = \frac{1}{x}\frac{\partial a_h}{\partial x}\frac{\partial}{\partial \xi}\ . \tag{24}$$

Then, in the semi-ideal limit (see Eq.(19) and (20)), the governing equations (13), (14) and (15) can be written in the following form:

$$\tilde{b_\vartheta} = \tilde{u_r}\, x\, (R_* < b_\vartheta >)\ , \tag{25}$$

$$\frac{\partial}{\partial\tau}(R_* < b_\vartheta >) + \frac{\partial}{\partial x}(< u_r > (R_* < b_\vartheta >)) = \frac{\partial}{\partial x}(\frac{< b_\vartheta >}{x})\ , \tag{26}$$

$$\frac{\partial < b_\vartheta >}{\partial\tau} + \frac{\partial < u_r b_\vartheta >}{\partial x} = 0\ . \tag{27}$$

Here $R_*(x,\tau) \equiv \dfrac{R_m}{2}\,(1-q)$ is a modified local magnetic Reynolds number with the "naive" q value defined as $q = \dfrac{\epsilon x < b_z >}{< b_\vartheta >}$. The averaging procedure $< \cdot >$ is defined in a usual way, $< \cdot > \equiv \dfrac{1}{2\pi}\displaystyle\int_0^{2\pi} (\cdot) d\xi$.

Note, that only the combination $(b_\vartheta - \epsilon x b_z)$ is a function of helical flux a_h (see Eqs.(22) and (24)) while b_ϑ can not be a constant on the magnetic surface $a_h = const$. This means that the "toroidal" current density and helical flux can evolve separatly from each other, eventhough the case of zero-beta plasma is considered (both the quantities will evolve together only if a force-free equilibrium is realized at every moment of time).

The relationship (25) between $\tilde{b_\vartheta}$ and $\tilde{u_r}$ follows directly from Eq.(13) and corresponds to the condition that the dissipative and flow-induced perturbations of radial magnetic field compensate each other. Note that Eq.(25) is equivalent to Eq.(16).

Eq.(26) describes resistive, of the order of $R_m^* \sim O(1)$, evolution of the "naive" q profile (actually, of the $(\mathbf{b} \cdot \nabla)$ amplitude) which takes place even in the absence of plasma flow. Of course, in the last case, b_ϑ and b_z evolve separately from each other on "slow" resistive time scale (see Eq.(14) and (15)). But their difference $\mid b_\vartheta - \epsilon x b_z \mid \sim \mid (\mathbf{b} \cdot \nabla) \mid \sim (1-q)$, which is initially small, can be strongly, in the relative sense of $\delta(1-q) \sim (1-q)$, disturbed on the ideal fast time scale. Eq.(26) is, thus, the equation for the combination $(b_\vartheta - \epsilon x b_z)$ multiplied by the factor R_m. The r.h.s. of Eq.(26) is the only term in the corresponding combination of the r.h.s. of Eqs.(14) and (15) which survives in the limit $(1-q) \to 0$.

Eq.(27) describes the $< b_\vartheta >$ dynamics (in the limit $(1-q) \to 0$ the $< b_\vartheta >$ and $< b_z >$ dynamics are closely related) which is akin to the "ideal" one with the averaged radial convective flux $< u_r b_\vartheta > \equiv < u_r >< b_\vartheta > + < \tilde{u_r} \tilde{b_\vartheta} >$. When we assume that the plasma flow makes a helical shift with $< u_r >= 0$ (this assumption is quite reasonable at the non-linear stage of a kink instability), it is known that the convective flux is controlled by the poloidally varying components $\tilde{u_r}$ and $\tilde{b_\vartheta}$ only. Taking into account the relationship (25), one thus obtains:

$$< u_r b_\vartheta > = < \tilde{u_r} \tilde{b_\vartheta} > = < \tilde{u_r}^2 > \; x \; (R_* < b_\vartheta >) \, . \tag{28}$$

After substitution of Eq.(28) into Eq.(27), a closed set of two equations for two unknown functions $(R_* < b_\vartheta >)$ and $< b_\vartheta >$ is obtained:

$$\frac{\partial}{\partial \tau}(R_* < b_\vartheta >) \; = \; \frac{\partial}{\partial x}\left(\frac{< b_\vartheta >}{x}\right) , \tag{29}$$

$$\frac{\partial < b_\vartheta >}{\partial \tau} \; + \; \frac{\partial}{\partial x}[< \tilde{u_r}^2 > \; x \; (R_* < b_\vartheta >)] \; = \; 0 \, . \tag{30}$$

Note that in terms of kinematic approach, which is used in this paper, any characteristic of plasma flow, say, $< \tilde{u_r}^2 >$ in Eq.(30), is treated as an externally defined function of radius and time. The only restriction on $\tilde{u_r}$, which follows from Eqs.(14) and (16), appears in the order of $O(\epsilon^2)$, so that $< \tilde{u_r}^2 >$ can be really considered as a free function in the main order of semi-ideal approach. Let it be a constant, like in the case of helical shift, i.e. $< \tilde{u_r}^2 >= u_0^2$ (such an assumption does not qualitatively change the physics of the flattening phenomenon but helps to simplify a problem). Using this approximation, one obtains from Eq.(29) and (30):

$$\frac{\partial^2 F}{\partial \tau^2} + \frac{u_0^2}{x} \frac{\partial}{\partial x}(x \frac{\partial F}{\partial x}) = 0 , \tag{31}$$

where $F(x, \tau) \equiv \dfrac{< b_\vartheta >}{x}$ (a flattened current density profile corresponds to a flattened radial distribution of the F value). Note, that Eq.(31) does not contain the resistive terms and describes an ideal dynamics of the $< b_\vartheta >$ governed by plasma flow. This explains the fact that the "toroidal" current density profile can be changed on the fast time scale. At first glance, this reminds the Wesson's result [7]. Actually, unlike to the Wesson's model, Eqs.(29) and (30) correspond to undisturbed ($b_r = 0$) magnetic surface and describe essentially resistive process of magnetic reconnection enhanced by the effect of a small $(1 - q)$.

Eq.(31) can be easily solved in terms of the Bessel function, but a formal solution can probably contain a singularity (this equation is of the elliptic type, and both the "boundary" conditions for time-coordinate are given at the same moment $\tau = 0$). Generally, if the initial $< b_\vartheta >$ and $\dfrac{\partial < b_\vartheta >}{\partial \tau}$ radial profiles are not properly adjusted, it could formally lead to an exponential growth of Bessel's harmonics, $\exp(u_0 \mu_k \tau) \cdot J_0(\mu_k x)$, where μ_k is the k-th zero of Bessel function J_0. But, actually, dissipative terms of the order of $\dfrac{\mu_k^2}{R_m}$, which are neglected in Eqs.(29) and (30), can be large enough at large μ_k value. Hence, Eq.(31) is valid only for the first few harmonics with $\mu_k \ll \sqrt{R_m}$, while higher harmonics are effectively suppressed by resistivity even on the fast "ideal" time scale $\tau \approx 1$. In the range of parameters corresponding to [1], only the first two harmonics really control the evolution of $< b_\vartheta >$ and, hence, current density profiles. During this evolution, which occurs on the fast time scale $\tau \approx (u_0\mu_1)^{-1}$, current density near the axis monotonically decreases (it follows from Eq.(30) with help of the fact that $(1-q)$ is a positive value), i.e. the current density profile tends to be a flattened one. Simultaneously, the shape of magnetic surfaces is undisturbed because the case with $b_r \equiv 0$ is considered. Thus, the proposed theoretical model of current profile flattening can qualitatively resolve the most important seemingly contradictory feature of the numerical simulation by Watanabe et al.

4. CONCLUSIONS

The present analysis shows that slightly non-ideal MHD evolution of magnetic configuration with the field lines nearly parallel to the direction of helical symmetry exhibits a multi-scale process characterized by the semi-ideal ordering, i.e., $R_m \to \infty$, $(1-q) \to 0$, $R_m^* \sim O(1)$ and $\mid b_r \mid \ll (1-q) \mid b_\vartheta \mid$. This ordering self-consistently contains two effects with well separated length and time scales. On one hand, poloidal and toroidal components of magnetic field are frozen into a plasma flow because of large ordinary magnetic Reynolds number $R_m \gg 1$. Consequently, their dynamics is controlled by radial convective flux, i.e. by plasma velocity. On the other hand, magnetic field is not completely frozen into the flow, in spite of large R_m value. This is because its dissipative slipping from an "ideal" magnetic surface can be cancelled by a flow-induced deformation of the surface. Such a cancellation is possible when $R_m\,(1-q) = R_m^* \sim 1$.

The semi-ideal behaviour is replaced by the ideal one if the angle between magnetic field lines and symmetry direction is not sufficiently small, i.e. $\mid 1-q \mid > \dfrac{1}{R_m}$ for $R_m \gg 1$. In this case field lines are frozen into plasma flow and, hence, magnetic surfaces are significantly deformed by the flow. On the other hand, the semi-ideal behaviour is replaced by the "resistive" one if $R_m \leq 1$. In this case plasma flow does not play any significant role in the evolution of magnetic configuration which is characterized by the "resistive" time scale τ_η . In conclusion, the semi-ideal evolution of magnetic configuration corresponds to a rather special case which is quite natural for the central part of plasma column (inside $q = 1$ magnetic surface) during the nonlinear evolution of $(m = 1/n = 1)$ kink mode.

ACKNOWLEDGEMENT

This paper is supported by Grants-in-Aid of the Ministry of Education, Science and Culture in Japan (No. 06044238 and No. 05836038).

References

[1]. K.Watanabe, T.Sato and Y.Nakayama, Nuclear Fusion, v.35, n.3, 251 (1995).

[2]. H.Soltwisch, Rev.Sci.Instrum., v.59, 1599 (1988).

[3]. W.P.West, D.M.Thomas, J.S.DeGrassie, and S.M.Zhang, Phys.Rev.Lett., v.58, 2758 (1987).

[4]. J.O'Rourke, Plasma Phys. Controlled Fusion, v.33, 289 (1991).

[5]. S.Migliuolo, Nuclear Fusion, v.33, n.11, 1721 (1993).

[6]. G.Ara, B.Basu, B.Coppi et al, Annals of Physics, v.112, 443 (1978).

[7]. J.A.Wesson, Plasma Phys. Controlled Fusion, v.28, 243 (1986).

Figure Captions

Fig.1.- Flattening of the averaged toroidal current density profile (simulation results from [1]).

Fig.2.- Simulation results [1] for the moment of time corresponding to a flattened current density profile:

(a) - intersections of magnetic field lines with the plane of a constant toroidal coordinate.

(b) - contours of a constant toroidal current density value;

(c) - projection of plasma flow on the plane of a constant toroidal coordinate;

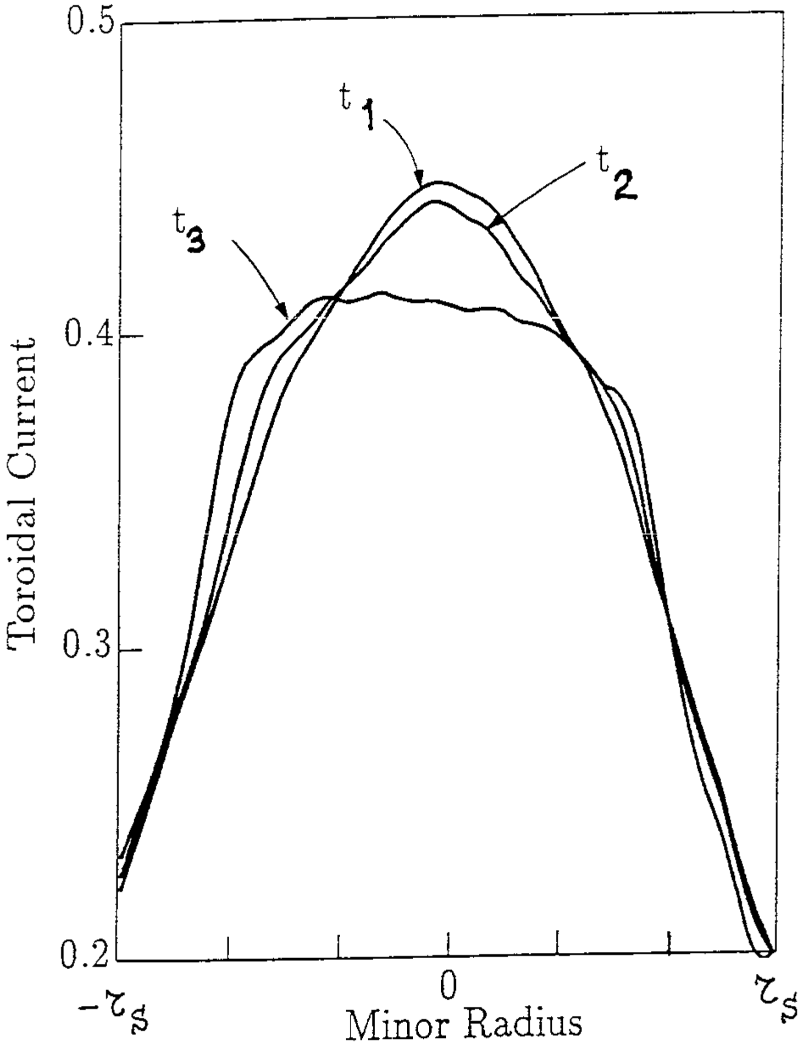

Fig. 1

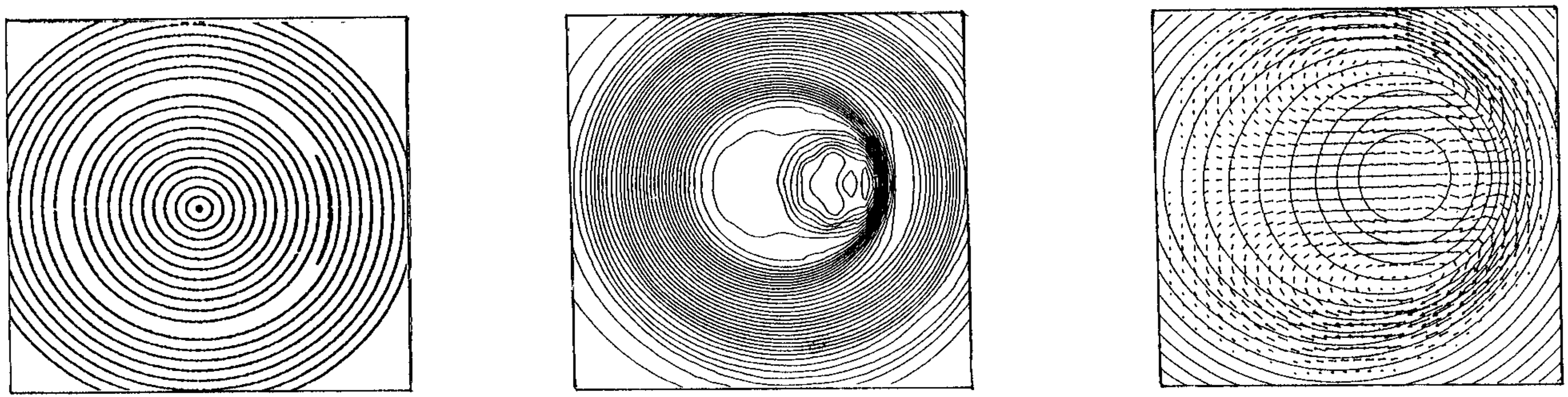

a) b) c)

Fig. 2

Recent Issues of NIFS Series

NIFS-328 V.D. Pustovitov,
Effect of Satellite Helical Harmonics on the Stellarator Configuration; Dec. 1994

NIFS-329 K. Itoh, S-I. Itoh and A. Fukuyama,
A Model of Sawtooth Based on the Transport Catastrophe; Dec. 1994

NIFS-330 K. Nagasaki, A. Ejiri,
Launching Conditions for Electron Cyclotron Heating in a Sheared Magnetic Field; Jan. 1995

NIFS-331 T.H. Watanabe, Y. Todo, R. Horiuchi, K. Watanabe, T. Sato,
An Advanced Electrostatic Particle Simulation Algorithm for Implicit Time Integration; Jan. 1995

NIFS-332 N. Bekki and T. Karakisawa,
Bifurcations from Periodic Solution in a Simplified Model of Two-dimensional Magnetoconvection; Jan. 1995

NIFS-333 K. Itoh, S.-I. Itoh, M. Yagi, A. Fukuyama,
Theory of Anomalous Transport in Reverse Field Pinch; Jan. 1995

NIFS-334 K. Nagasaki, A. Isayama and A. Ejiri
Application of Grating Polarizer to 106.4GHz ECH System on Heliotron-E; Jan. 1995

NIFS-335 H. Takamaru, T. Sato, R. Horiuchi, K. Watanabe and Complexity Simulation Group,
A Self-Consistent Open Boundary Model for Particle Simulation in Plasmas; Feb. 1995

NIFS-336 B.B. Kadomtsev,
Quantum Telegragh : is it possible?; Feb. 1995

NIFS-337 B.B.Kadomtsev,
Ball Lightning as Self-Organization Phenomenon; Feb. 1995

NIFS-338 Y. Takeiri, A. Ando, O. Kaneko, Y. Oka, K. Tsumori, R. Akiyama, E. Asano, T. Kawamoto, M. Tanaka and T. Kuroda,
High-Energy Acceleration of an Intense Negative Ion Beam; Feb. 1995

NIFS-339 K. Toi, T. Morisaki, S. Sakakibara, S. Ohdachi, T.Minami, S. Morita, H. Yamada, K. Tanaka, K. Ida, S. Okamura, A. Ejiri, H. Iguchi, K. Nishimura, K. Matsuoka, A. Ando, J. Xu, I. Yamada, K. Narihara, R. Akiyama, H. Idei, S. Kubo, T. Ozaki, C. Takahashi, K. Tsumori,
H-Mode Study in CHS; Feb. 1995

NIFS-340 T. Okada and H. Tazawa,
Filamentation Instability in a Light Ion Beam-plasma System with External Magnetic Field; Feb. 1995

NIFS-341 T. Watanbe, G. Gnudi,
A New Algorithm for Differential-Algebraic Equations Based on HIDM; Feb. 13, 1995

NIFS-342 Y. Nejoh,
New Stationary Solutions of the Nonlinear Drift Wave Equation; Feb. 1995

NIFS-343 A. Ejiri, S. Sakakibara and K. Kawahata,
Signal Based Mixing Analysis for the Magnetohydrodynamic Mode Reconstruction from Homodyne Microwave Reflectometry; Mar.. 1995

NIFS-344 B.B.Kadomtsev, K. Itoh, S.-I. Itoh
Fast Change in Core Transport after L-H Transition; Mar. 1995

NIFS-345 W.X. Wang, M. Okamoto, N. Nakajima and S. Murakami,
An Accurate Nonlinear Monte Carlo Collision Operator; Mar. 1995

NIFS-346 S. Sasaki, S. Takamura, S. Masuzaki, S. Watanabe, T. Kato, K. Kadota,
Helium I Line Intensity Ratios in a Plasma for the Diagnostics of Fusion Edge Plasmas; Mar. 1995

NIFS-347 M. Osakabe,
Measurement of Neutron Energy on D-T Fusion Plasma Experiments; Apr. 1995

NIFS-348 M. Sita Janaki, M.R. Gupta and Brahmananda Dasgupta,
Adiabatic Electron Acceleration in a Cnoidal Wave; Apr. 1995

NIFS-349 J. Xu, K. Ida and J. Fujita,
A Note for Pitch Angle Measurement of Magnetic Field in a Toroidal Plasma Using Motional Stark Effect; Apr. 1995

NIFS-350 J. Uramoto,
Characteristics for Metal Plate Penetration of a Low Energy Negative Muonlike or Pionlike Particle Beam: Apr. 1995

NIFS-351 J. Uramoto,
An Estimation of Life Time for A Low Energy Negative Pionlike Particle Beam: Apr. 1995

NIFS-352 A. Taniike,
Energy Loss Mechanism of a Gold Ion Beam on a Tandem Acceleration System: May 1995

NIFS-353 A. Nishizawa, Y. Hamada, Y. Kawasumi and H. Iguchi,
Increase of Lifetime of Thallium Zeolite Ion Source for Single-Ended Accelerator: May 1995

NIFS-354 S. Murakami, N. Nakajima, S. Okamura and M. Okamoto,
Orbital Aspects of Reachable β Value in NBI Heated Heliotron/Torsatrons; May 1995

NIFS-355 H. Sugama and W. Horton,
Neoclassical and Anomalous Transport in Axisymmetric Toroidal Plasmas with Electrostatic Turbulence; May 1995

NIFS-356 N. Ohyabu
A New Boundary Control Scheme for Simultaneous Achievement of H-mode and Radiative Cooling (SHC Boundary); May 1995

NIFS-357 Y. Hamada, K.N. Sato, H. Sakakita, A. Nishizawa, Y. Kawasumi, R. Liang, K. Kawahata, A. Ejiri, K. Toi, K. Narihara, K. Sato, T. Seki, H. Iguchi, A. Fujisawa, K. Adachi, S. Hidekuma, S. Hirokura, K. Ida, M. Kojima, J. Koong, R. Kumazawa, H. Kuramoto, T. Minami,. M. Sasao, T. Tsuzuki, J.Xu, I. Yamada, and T. Watari,
Large Potential Change Induced by Pellet Injection in JIPP T-IIU Tokamak Plasmas; May 1995

NIFS-358 M. Ida and T. Yabe,
Implicit CIP (Cubic-Interpolated Propagation) Method in One Dimension; May 1995

NIFS-359 A. Kageyama, T. Sato and The Complexity Simulation Group,
Computer Has Solved A Historical Puzzle: Generation of Earth's Dipole Field; June 1995

NIFS-360 K. Itoh, S.-I. Itoh, M. Yagi and A. Fukuyama,
Dynamic Structure in Self-Sustained Turbulence; June 1995

NIFS-361 K. Kamada, H. Kinoshita and H. Takahashi,
Anomalous Heat Evolution of Deuteron Implanted Al on Electron Bombardment; June 1995

NIFS-362 V.D. Pustovitov,
Suppression of Pfirsch-schlüter Current by Vertical Magnetic Field in Stellarators: June 1995

NIFS-363 A. Ida, H. Sanuki and J. Todoroki
An Extended K-dV Equation for Nonlinear Magnetosonic Wave in a Multi-Ion Plasma; June 1995

NIFS-364 H. Sugama and W. Horton
Entropy Production and Onsager Symmetry in Neoclassical Transport

Processes of Toroidal Plasmas; July 1995

NIFS-365 K. Itoh, S.-I. Itoh, A. Fukuyama and M. Yagi,
On the Minimum Circulating Power of Steady State Tokamaks; July 1995

NIFS-366 K. Itoh and Sanae-I. Itoh,
The Role of Electric Field in Confinement; July 1995

NIFS-367 F. Xiao and T. Yabe,
A Rational Function Based Scheme for Solving Advection Equation; July 1995

NIFS-368 Y. Takeiri, O. Kaneko, Y. Oka, K. Tsumori, E. Asano, R. Akiyama, T. Kawamoto and T. Kuroda,
Multi-Beamlet Focusing of Intense Negative Ion Beams by Aperture Displacement Technique; Aug. 1995

NIFS-369 A. Ando, Y. Takeiri, O. Kaneko, Y. Oka, K. Tsumori, E. Asano, T. Kawamoto, R. Akiyama and T. Kuroda,
Experiments of an Intense H- Ion Beam Acceleration; Aug. 1995

NIFS-370 M. Sasao, A. Taniike, I. Nomura, M. Wada, H. Yamaoka and M. Sato,
Development of Diagnostic Beams for Alpha Particle Measurement on ITER; Aug. 1995

NIFS-371 S. Yamaguchi, J. Yamamoto and O. Motojima;
A New Cable -in conduit Conductor Magnet with Insulated Strands; Sep. 1995

NIFS-372 H. Miura,
Enstrophy Generation in a Shock-Dominated Turbulence; Sep. 1995

NIFS-373 M. Natsir, A. Sagara, K. Tsuzuki, B. Tsuchiya, Y. Hasegawa, O. Motojima,
Control of Discharge Conditions to Reduce Hydrogen Content in Low Z Films Produced with DC Glow; Sep. 1995

NIFS-374 K. Tsuzuki, M. Natsir, N. Inoue, A. Sagara, N. Noda, O. Motojima, T. Mochizuki, I. Fujita, T. Hino and T. Yamashina,
Behavior of Hydrogen Atoms in Boron Films during H_2 *and He Glow Discharge and Thermal Desorption;* Sep. 1995

NIFS-375 U. Stroth, M. Murakami, R.A. Dory, H. Yamada, S. Okamura, F. Sano and T. Obiki,
Energy Confinement Scaling from the International Stellarator Database; Sep. 1995